ELSEVIER

Journal of Neuroscience Methods 105 (2001) 65–75

JOURNAL OF NEUROSCIENCE METHODS

www.elsevier.com/locate/jneumeth

Wavelet entropy: a new tool for analysis of short duration brain electrical signals

Osvaldo A. Rosso [a,*], Susana Blanco [a], Juliana Yordanova [b], Vasil Kolev [b], Alejandra Figliola [a], Martin Schürmann [c], Erol Başar [c,d]

[a] *Facultad de Ciencias Exactas y Naturales, Instituto de Cálculo, Universidad de Buenos Aires, Pabellón II, Ciudad Universitaria, 1428 Buenos Aires, Argentina*

[b] *Institute of Physiology, Bulgarian Academy of Sciences, Acad. G. Bonchev Str., bl. 23, 1113 Sofia, Bulgaria*

[c] *Institute of Physiology, Medical University Lübeck, Ratzeburger Alle 160, D-23538 Lübeck, Germany*

[d] *TÜBITAK Brain Dynamics Research Unit, Ankara, Turkey*

Received 12 June 2000; received in revised form 31 October 2000; accepted 31 October 2000

Abstract

Since traditional electrical brain signal analysis is mostly qualitative, the development of new quantitative methods is crucial for restricting the subjectivity in the study of brain signals. These methods are particularly fruitful when they are strongly correlated with intuitive physical concepts that allow a better understanding of brain dynamics. Here, new method based on orthogonal discrete wavelet transform (ODWT) is applied. It takes as a basic element the ODWT of the EEG signal, and defines the relative wavelet energy, the wavelet entropy (WE) and the relative wavelet entropy (RWE). The relative wavelet energy provides information about the relative energy associated with different frequency bands present in the EEG and their corresponding degree of importance. The WE carries information about the degree of order/disorder associated with a multi-frequency signal response, and the RWE measures the degree of similarity between different segments of the signal. In addition, the time evolution of the WE is calculated to give information about the dynamics in the EEG records. Within this framework, the major objective of the present work was to characterize in a quantitative way functional dynamics of order/disorder microstates in short duration EEG signals. For that aim, spontaneous EEG signals under different physiological conditions were analyzed. Further, specific quantifiers were derived to characterize how stimulus affects electrical events in terms of frequency synchronization (tuning) in the event related potentials. © 2001 Published by Elsevier Science B.V.

Keywords: EEG, event-related potentials (ERP); Visual evoked potential; Time–frequency signal analysis; Wavelet analysis; Signal entropy

1. Introduction

Recently, oscillatory electroencephalographic (EEG) activity has been discussed in relation with functional neuronal mechanisms. In this regard, it is of major interest to investigate how brain electric oscillations get synchronized during pathological or physiological brain states (e.g. epileptic seizures, sleep-wake stages, etc.), or by external and internal stimulation. This issue can be addressed by applying methods of system analysis to the EEG signals, because changes in EEG activity occur in temporal relation to triggering events, and correspond to transitions from disordered to ordered states, or vice versa.

The EEG can be regarded as reflecting the activity of ensembles of generators producing oscillations in several frequency ranges, which are active in a very complex manner. Upon stimulation they begin to act together in a coherent way. This transition from a disordered to an ordered state is accompanied by a resonance phenomenon and results in frequency stabilization, synchronization, and enhancement of the ongoing EEG activity, which produces event-related brain potentials (ERPs, Sayers et al., 1974; Başar, 1980, 1998, 1999). Although different methods have provided indirect evidence for synchronization EEG processes (Başar, 1980; Abarbanel, 1996), a tool for a quantita-

* Corresponding author. Tel.: +54-11-4576-3375; fax: +54-11-4786-8114.

E-mail address: rosso@ulises.ic.fcen.uba.ar (O.A. Rosso).

0165-0270/01/$ - see front matter © 2001 Published by Elsevier Science B.V.
PII: S0165-0270(00)00356-3

tive evaluation of the complex EEG signal synchronization and its temporal dynamics is still lacking.

In the characterization of the time evolution of complex EEG dynamics, quantifiers based on nonlinear dynamics have been previously applied. They analyze the temporal evolution of the EEG signal complexity (associated with the measurement of the correlation dimension D_2, Casdagli et al., 1997; Lehnertz and Elger, 1998) and the degree of chaoticness (in terms of the largest Lyapunov exponent, Λ_{max}, Iasemedis et al., 1990; Iasemedis and Sackellares, 1991). For example, when applied to EEG epileptic time series, a transition from a complex behavior of the neural network to a simpler one could be detected at or even before seizure onset (Iasemedis et al., 1990; Iasemedis and Sackellares, 1991; Pjin et al., 1991; Lehnertz and Elger, 1998). Despite the apparent physiological relevance of such findings, a basic requirement for the application of nonlinear dynamics metric tools (chaos theory) is the stationarity of the time series, which suggests that the time series represent a unique and stable attractor. Also, for the evaluation of D_2 and Λ_{max} defined as asymptotic properties of the attractor, long time recordings are required. This is a serious restriction for investigation of short duration brain electrical signals like ERPs. Moreover, these metric invariants require the computation of primary parameters that rapidly degrade with additive noise (for a review see Elbert et al., 1994; Abarbanel, 1996; Başar, 1998).

Alternatively, a natural approach to quantify the degree of order of a complex signal is to consider its spectral entropy, as defined from the Fourier power spectrum (Powell and Percival, 1979). The spectral entropy is a measure of how concentrated or widespread the Fourier power spectrum of a signal is. An ordered activity, like a sinusoidal signal, is manifested as a narrow peak in the frequency domain. This concentration of the frequency spectrum in one single peak corresponds to a low entropy value. On the other extreme, a disordered activity (e.g. the one generated by pure noise or by a deterministic chaotic system) will have a wide band response in the frequency domain, thus being reflected in higher entropies.

Inouye et al. (1991, 1993) first applied the spectral entropy to study brain electrical signals. However, the applicability of this method to short lasting and nonstationary data segments (such as ERPs) has restrictions. The Fourier transform (FT) requires stationarity of the signal, the EEG being highly nonstationary. Furthermore, FT does not give the time evolution of the frequency patterns, and in consequence, the spectral entropy is not defined as a function of time.

The disadvantages of the spectral entropy defined from the FT can be partially resolved by using a short time Fourier transform (STFT). Powell and Percival (1979) defined a time evolving entropy from STFT by using a Hanning window. With this approach, FT is applied to time-evolving windows of a few seconds of data refined with an appropriate function. Then, the evolution of the frequencies can be followed and the stationary requirement is partially satisfied by considering the signals as quasi-stationary for a few seconds. Due to the uncertainty principle, one critical limitation appears when windowing data, if the window is too narrow, the frequency resolution will be poor; and if the window is too wide, the time localization will be less precise. This limitation becomes important when the signal has transient components localized in time such as ERP components.

To overcome these limitations a time evolving entropy can be defined from a time–frequency representation of the signal as provided by the wavelet transform (WT, Blanco et al., 1998; Quian Quiroga et al., 2000a). The orthogonal discrete wavelet transform (ODWT) makes no assumptions about record stationarity and the only input needed is the time series (Blanco et al., 1995, 1996, 1998). In this case, the time evolution of frequency patterns can be followed with an optimal time–frequency resolution. Therefore, while entropy based on the WT reflects the degree of order/disorder of the signal, it can provide additional information about the underlying dynamical process associated with the signal (Rosso and Blanco, 1999).

Within this framework, the major objective of the present work was to characterize in a quantitative way functional dynamics of order/disorder microstates in short duration EEG signals. (i) One aim was to demonstrate the applicability of WE measures to analysis of short segments of spontaneous EEG. This application may turn especially useful for studying EEG synchronization in conditions with certain limitations for long duration records, as for example in clinical cases, children, etc. (ii) A second aim was to analyze quantitatively complex signal synchronization processes in ERPs. It was of particular interest to show how stimulus affects electrical events in terms of EEG frequency synchronization or tuning. Stimulus information processing may vary with specific sensory/cognitive processing demands (Gazzaniga et al., 1998). Thus, identifying temporal and spatial regions of synchrony/desynchrony by describing the temporal evolution of WE in different task conditions was of major relevance.

In the present work, using the ODWT of the EEG, three parameters were defined, (1) relative wavelet energy, (2) WE, and (3) relative wavelet entropy (RWE). The relative wavelet energy is introduced to provide information about the relative energy associated with the different frequency bands present in the EEG/ERP segments. The WE is used to characterize the degree of order/disorder associated with a multi-frequency signal response, and the RWE is measured to reflect the degree of similarity between different segments of the

signal. To characterize precisely order/disorder microstates in short lasting ERPs and their timing, specific quantifiers were derived and applied.

2. Methods

2.1. Wavelet transform

The wavelet analysis is a method, which relies on the introduction of an appropriate basis and a characterization of the signal by the distribution of amplitude in the basis. If the wavelet is required to form a proper orthogonal basis, it has the advantage that an arbitrary function can be uniquely decomposed and the decomposition can be inverted (Daubechies, 1992; Aldroubi and Unser, 1996; Mallat, 1999).

The *wavelet* is a smooth and quickly vanishing oscillating function with good localization in both frequency and time. A *wavelet family* $\psi_{a,b}$ is the set of elementary functions generated by dilations and translations of a unique admissible *mother wavelet* $\psi(t)$:

$$\psi_{a,b}(t) = |a|^{-1/2}\psi\left(\frac{t-b}{a}\right), \tag{1}$$

where $a,b \in \mathscr{R}$, $a \neq 0$ are the scale and translation parameters, respectively, and t is the time. As a increases, the wavelet becomes narrower. Thus, one have a unique analytic pattern and its replications at different scales and with variable time localization.

The *continuous wavelet transform* (CWT) of a signal $S(t) \in L^2(\mathscr{R})$ (the space of real square summable functions) is defined as the correlation between the function $S(t)$ with the family wavelet $\psi_{a,b}$ for each a and b:

$$(W_\psi S)(a,b) = |a|^{-1/2}\int_{-\infty}^{\infty} S(t)\psi^*\left(\frac{t-b}{a}\right)\mathrm{d}t = \langle S, \psi_{a,b}\rangle. \tag{2}$$

For special election of the mother wavelet function $\psi(t)$ and for the discrete set of parameters, $a_j = 2^{-j}$ and $b_{j,k} = 2^{-j}k$, with j, $k \in Z$ (the set of integers) the family

$$\psi_{j,k}(t) = 2^{j/2}\psi(2^j t - k) \quad j,k \in Z \tag{3}$$

constitutes an orthonormal basis of the Hilbert space $L^2(\mathscr{R})$ consisting of finite-energy signals. The correlated *decimated discrete wavelet transform* (DWT) provides a nonredundant representation of the signal and its values constitute the coefficients in a wavelet series. These wavelet coefficients provide full information in a simple way and a direct estimation of local energies at the different scales. Moreover, the information can be organized in a hierarchical scheme of nested subspaces called multiresolution analysis in $L^2(\mathscr{R})$. In the present work, we employ orthogonal cubic spline functions as mother wavelets. Among several alternatives, cubic spline functions are symmetric and combine in a suitable proportion smoothness with numerical advantages and they have become a recommendable tool for representing natural signals.

In the following, the signal is assumed to be given by the sampled values $S = \{s_0(n),\ n = 1,\ \ldots,\ M\}$, corresponding to an uniform time grid with sampling time t_s. For simplicity the sampling rate is taken as $t_s = 1$. If the decomposition is carried out over all resolutions levels, $N = \log_2(M)$, the wavelet expansion will be:

$$S(t) = \sum_{j=-N}^{-1}\sum_k C_j(k)\psi_{j,k}(t) = \sum_{j=-N}^{-1} r_j(t), \tag{4}$$

where wavelet coefficients $C_j(k)$ can be interpreted as the local residual errors between successive signal approximations at scales j and $j+1$, and $r_j(t)$ is the *residual signal* at scale j. It contains the information of the signal $S(t)$ corresponding to the frequencies $2^{j-1}\omega_s \leq |\omega| \leq 2^j\omega_s$.

2.2. Relative wavelet energy

Since the family $\{\psi_{j,k}(t)\}$ is an *orthonormal* basis for $L^2(\mathscr{R})$, the concept of energy is linked with the usual notions derived from the Fourier theory. Then, the wavelet coefficients are given by $C_j(k) = \langle S,\psi_{j,k}\rangle$, the energy at each resolution level $j = -1,\ \ldots,\ -N$, will be the energy of the detail signal

$$E_j = \|r_j\|^2 = \sum_k |C_j(k)|^2, \tag{5}$$

and the energy at each sampled time k will be

$$E(k) = \sum_{j=-N}^{-1} |C_j(k)|^2. \tag{6}$$

In consequence, the total energy can be obtained by

$$E_{\mathrm{tot}} = \|S\|^2 = \sum_{j<0}\sum_k |C_j(k)|^2 = \sum_{j<0} E_j. \tag{7}$$

Then, the normalized values, which represent the *relative wavelet energy*,

$$p_j = \frac{E_j}{E_{\mathrm{tot}}} \tag{8}$$

for the resolution level $j = -1,\ -2,\ \ldots,\ -N$, define by scales the probability distribution of the energy. Clearly, $\Sigma_j p_j = 1$ and the distribution $\{p_j\}$ can be considered as a time–scale density. This gives a suitable tool for detecting and characterizing specific phenomena in time and frequency planes.

2.3. Wavelet entropy

2.3.1. Total wavelet entropy

The Shannon entropy (Shannon, 1948) gives an useful criterion for analyzing and comparing probability distribution, it provides a measure of the information

of any distribution. We define the total WE (Blanco et al., 1998) as

$$S_{WT} \equiv S_{WT}(p) = -\sum_{j<0} p_j \cdot \ln[p_j]. \quad (9)$$

The WE appears as a measure of the degree of order/disorder of the signal, so it can provide useful information about the underlying dynamical process associated with the signal. In fact, a very ordered process could be thought of as a periodic mono-frequency signal (signal with a narrow band spectrum). A wavelet representation of such a signal will be greatly resolved in one unique wavelet resolution level, i.e. all relative wavelet energies will be almost zero except for the wavelet resolution level which includes the representative signal frequency. For this special level the relative wavelet energy will be almost one and in consequence the total WE will be near zero or of a very low value. A signal generated by a totally random process can be taken as representing a very disordered behavior. This kind of a signal will have a wavelet representation with significant contributions from all frequency bands. Moreover, one could expect that all the contributions will be of the same order. Consequently, the relative wavelet energy will be almost equal for all resolution levels and the WE will take their maximum values.

2.3.2. Relative wavelet entropy

Let us now suppose that we have two different probability distributions $\{p_j\}$ and $\{q_j\}$, with $\Sigma_j p_j = \Sigma_j q_j = 1$. In this case, they can be thought of as representing by scales the probability distribution of the wavelet energy for two segments of a signal or of two different signals. We define the RWE, formally a Kullback–Leibler entropy (Gray, 1990; Guiasu, 1997; Quian Quiroga et al., 2000b), as:

$$S_{WT}(p|q) = \sum_{j<0} p_j \cdot \ln\left[\frac{p_j}{q_j}\right], \quad (10)$$

which gives a measure of the degree of similarity between two probability distributions (more precisely of distribution $\{p_j\}$ with respect to the distribution $\{q_j\}$ taken as a reference distribution). Note that the RWE is positive and vanishes only if $p_j \equiv q_j$.

Fig. 1 presents three different relative wavelet energy (probability) distributions corresponding to five wavelet resolution levels ($j = -5, \ldots, -1$). It is clear from the figure that distributions **A** and **B** are quite similar, and present broad band spectra. In contrast, distribution **C** shows a clear dominance of the resolution level $j = -2$. According to the description given above, for the total WE the following relation can be expected: $S_{WT}(\mathbf{A}) \approx S_{WT}(\mathbf{B}) > S_{WT}(\mathbf{C})$. Taking, for example, the distribution **A** as reference, it can be expected for the RWE that: $S_{WT}(\mathbf{B}|\mathbf{A}) \simeq 0$ and $S_{WT}(\mathbf{C}|\mathbf{A}) \gg 0$. When the corresponding numerical values for the distributions are used, a very good agreement with the previous relations are obtained (Fig. 1).

2.3.3. Time evolution of total wavelet entropy and relative wavelet entropy

Eqs. (8)–(10) define useful quantifiers based on ODWT to make a quantitative EEG analysis. In order to study temporal evolution, the analyzed signal is divided in nonoverlapping temporal windows of length L and for each interval i ($i = 1, \ldots, N_T$, with $N_T = M/L$) relative wavelet energy, WE and RWE is evaluated. The obtained value is assigned to the central point of the time window. In case of diadic wavelet decomposition, at resolution level j the number of wavelet coefficients is two times smaller than in the previous ones. The minimum length of the temporal window will, therefore, include at least one wavelet coefficient in each scale.

In the present work, short duration brain electrical signals like ERPs are in the focus of interest. From a physiological point of view, it is well established that the major power of ERPs lies in the low frequency

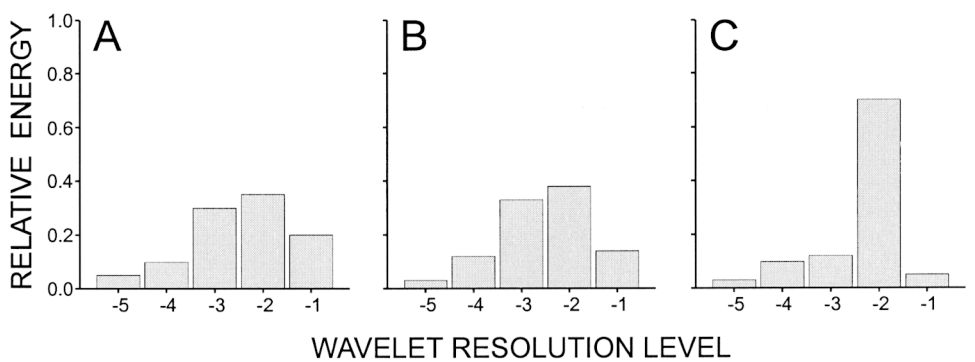

Fig. 1. Relative wavelet energy (probability) distributions corresponding to five wavelet resolution levels ($j = -5, \ldots, -1$). Distribution **A**, $\{p_j\} = \{0.05, 0.10, 0.30, 0.35, 0.20\}$; **B**, $\{p_j\} = \{0.03, 0.12, 0.33, 0.38, 0.14\}$; **C**, $\{p_j\} = \{0.03, 0.10, 0.12, 0.70, 0.05\}$. The WE values for these distributions are $S_{WT}(\mathbf{A}) = 1.430$, $S_{WT}(\mathbf{B}) = 1.368$ and $S_{WT}(\mathbf{C}) = 0.989$. Taking the distribution **A** as reference, $S_{WT}(\mathbf{B}|\mathbf{A}) = 0.019$ and $S_{WT}(\mathbf{C}|\mathbf{A}) = 0.291$.

bands (delta = 0.1–4 Hz, theta = 4–7 Hz and alpha = 8–13 Hz). This fact is taken into account for time evolution evaluation of relative wavelet energy, WE and RWE, by considering the mean wavelet energy instead of the total wavelet energy. The mean wavelet energy at resolution level j for the time window i is given by:

$$E_j^{(i)} = \frac{1}{N_j} \sum_{k=(i-1)L+1}^{i \cdot L} |C_j(k)|^2 \quad \text{with } i = 1, \ldots, N_T, \tag{11}$$

where N_j represents the number of wavelet coefficients at resolution level j included in the time interval i. Then the total mean energy at this time window will be:

$$E_{\text{tot}}^{(i)} = \sum_{j<0} E_j^{(i)}. \tag{12}$$

The time evolution of relative wavelet energy is defined as:

$$p_j^{(i)} = \frac{E_j^{(i)}}{E_{\text{tot}}^{(i)}}, \tag{13}$$

and the time evolution of WE and RWE will be given by:

$$S_{\text{WT}}^{(i)}(p) = -\sum_{j<0} p_j^{(i)} \cdot \ln[p_j^{(i)}], \tag{14}$$

$$S_{\text{WT}}^{(i)}(p|q) = \sum_{j<0} p_j^{(i)} \cdot \ln\left[\frac{p_j^{(i)}}{q_j^{(i)}}\right], \tag{15}$$

respectively.

2.4. Quantifiers based on relative wavelet energy, wavelet entropy, and relative wavelet entropy

To characterize in a quantitative way complex functional dynamics of short duration signals, a series of quantifiers based on the previous definitions is introduced.

2.4.1. Temporal average and mean wavelet entropy

In order to obtain a quantifier for the whole time period, in which the signal of interest emerges (e.g. background EEG, ictal EEG, post-stimulus EEG, etc.) the temporal average is evaluated. The temporal average of WE is given by

$$\langle S_{\text{WT}} \rangle = \frac{1}{N_T} \sum_{i=1}^{N_T} S_{\text{WT}}^{(i)} \tag{16}$$

and for the mean wavelet energy at resolution level j

$$\langle E_j \rangle = \frac{1}{N_T} \sum_{i=1}^{N_T} E_j^{(i)}; \tag{17}$$

then the total mean of wavelet energy temporal average is defined as

$$\langle E_{\text{tot}} \rangle = \sum_{j<0} \langle E_j \rangle. \tag{18}$$

In consequence, a mean probability distribution $\{q_j\}$ representative for the whole time interval can be defined as

$$q_j = \frac{\langle E_j \rangle}{\langle E_{\text{tot}} \rangle} \tag{19}$$

with $\Sigma_j q_j = 1$ and the corresponding mean WE as

$$\tilde{S}_{\text{WT}} = -\sum_{j<0} q_j \cdot \ln[q_j]. \tag{20}$$

2.4.2. Rate of wavelet entropy change

While evaluating ERP dynamics, it is of importance to consider the relative change of the event-related EEG against the background (or ongoing) EEG activity representing a reference. In the following, $t = 0$ is taken for the moment of stimulus occurrence. Then $\langle S_{\text{WT}} \rangle$ for the pre- ($t < 0$) and post-stimulus ($t > 0$) epochs is evaluated. $\tilde{S}_{\text{WT}}$ for the pre-stimulus EEG is also computed to be taken as a reference. In addition, the signal rate of WE change Γ (valid for time $t > 0$) is given by:

$$\Gamma = \left[\frac{S_{\text{WT}}^{(i)} - \tilde{S}_{\text{WT}}^{(\text{pre})}}{\tilde{S}_{\text{WT}}^{(\text{pre})}}\right] 100\%. \tag{21}$$

$\Gamma < 0$ ($\Gamma > 0$) implies that post-stimulus signal shows a higher degree of order (disorder) than the reference EEG signal, and its value presents the difference between the two epochs in percents.

2.4.3. Time localizations

Two latency parameters, denoted by t_{m} and t_{M}, are also introduced. The first one, the latency $t_{\text{m}} > 0$, represents the post-stimulus time in which total WE shows a minimum value. Therefore, this latency is associated with the time in which the stimulus induces the highest degree of frequency tuning in the brain electrical activity, which would produce the highest degree of order in the post-stimulus period. An example of ERP and t_{m} time localization is illustrated in Fig. 2.

The second latency $t_{\text{M}} > 0$ is defined as the post-stimulus time in which the RWE has a maximum value. At time t_{M}, the ERP and the reference EEG signal manifest a highest degree of nonsimilitude, which can be associated again in a causal way with the stimulus effect. An example of t_{M} time localization is shown in Fig. 2. In principle, these two latencies are expected to coincide, but this should be proved in each particular case under study. To quantify the corresponding signal behavior at these two latencies, $\Gamma[t_{\text{m}}]$ and $\Gamma[t_{\text{M}}]$ at t_{m} and t_{M}, respectively, are evaluated.

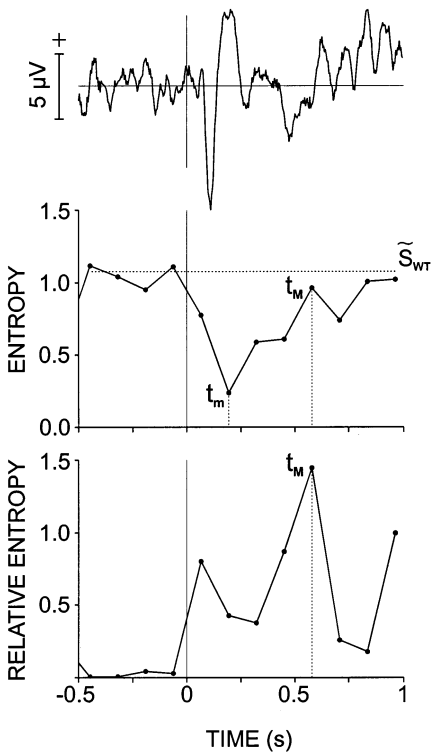

Fig. 2. EEG-ERP signal for a typical subject at Pz. Time evolution of total WE and RWE (central and bottom panels) show the latencies $t_m = 192$ ms (minimum value of the WE) and $t_M = 596$ ms (maximum value of the RWE). In the central panel, the horizontal line represents the mean WE for the background EEG epoch (reference) $\tilde{S}_{WT} = 1.076$, used to evaluate the signal rate of WE change $\Gamma(t_m) = -78.034\%$ and $\Gamma(t_M) = -10.405\%$ at these latencies.

3. Application

3.1. Experimental setup

3.1.1. Subjects

The experiments were carried out on 13 healthy volunteers aged between 22 and 25 years (mean age = 23.6 years), colleagues and students from the Medical University and the Free University, Sofia. None of them reported of any neurologic or psychiatric disorder or hearing problems in the past. Subjects were also drug-free during the experimental sessions.

3.1.2. Data recording and acquisition

The subjects sat in an electrically shielded, sound-diminished, and dimly illuminated room. For EEG data recording Ag–AgCl disc electrodes were placed on the mid-line frontal (Fz), central (Cz), and parietal (Pz) locations according to the International 10/20 system, and were referenced against linked earlobes. Electrode impedance was less than 5 kΩ. Electrooculogram (EOG) was also recorded to mark eye movement artifacts. The cut-off frequencies of the EEG amplifiers were set to 0.1 and 120 Hz. Bioelectrical signals were sampled with a frequency of 250 Hz (12 bit). Spontaneous EEG was recorded for 5 min during eyes closed and eye open conditions. For analysis, 30 consecutive artifact-free epochs were used, each of 2 s duration.

The epochs recorded for ERP analysis started at 1024 ms before and ended at 1024 ms after stimulus presentation. The stored raw single-sweeps were selected off-line to eliminate EEG segments contaminated with blink, muscular or any other type of artifact activity. Also, any EEG or EOG trial exceeding ± 50 μV was excluded from further analysis. Thus, the mean number of artifact-free sweeps analyzed for each subject in each series was 35.

3.1.3. Stimuli

The stimuli were tones with frequency of 800 Hz, intensity of 60 dB SPL, and duration of 50 ms (r/f 10 ms). Inter-stimulus intervals varied randomly in steps of 1 s between 3.5 and 5.5 s (mean 4.5 s).

3.1.4. Experimental paradigms

Two experimental conditions were applied. The first recording session was *a passive listening condition* (PLC), in which 50 identical auditory stimuli (800 Hz tones) were used. According to the instruction, subjects had to relax silently with closed eyes. The second experimental session was *a simple reaction task* (SRT). During the SRT, the same as in the PLC set of stimuli was presented, with subjects required to respond to each stimulus by pressing a push-button as fast as possible.

3.2. Data analysis

The wavelet multiresolution decomposition, described in the previous section, was used for decomposing the signals in scale levels defined in agreement with the traditional frequency bands derived by the clinical EEG analysis. After a five octave wavelet decomposition (in accordance with the sampling rate of 250 Hz), the components of the following frequency bands were obtained, 63–125 Hz ($j = -1$); 31–62 Hz ($j = -2$, gamma); 16–30 Hz ($j = -3$, beta); 8–15 Hz ($j = -4$, alpha); 4–8 Hz ($j = -5$, theta) and the residues in the 0.5–4 Hz band ($r = -5$, delta). Values of the residue can be used as a very good approximation of the wavelet coefficients representing delta frequency band. To simplify the notation, we represent it by $j = -6$ instead of $r = -5$. Note also that in this case, the number of coefficients of the level $j = -5$ is the same. In the present study, the traditional frequency bands are considered, i.e. the contributions of $j = -1$ are taken as null in the evaluation of the different quantifiers defined in previous section.

The ODWT was applied to each single sweep from each electrode and condition using cubic-spline func-

tion as a mother wavelet, thus obtaining the corresponding wavelet coefficients at time sample k: $C_j^{(n)}(k)$ within $j = -1, \ldots, -6$ and $n = 1, \ldots, N_s$ (N_s is the number of single-sweeps). Then, the final wavelet coefficients were obtained by averaging over single sweeps from each electrode and condition. The time evolution of relative wavelet energy, total WE and RWE (taking as reference the total pre-stimulus epoch) were evaluated with nonoverlapping time windows of length $L = 32$ *data points* = 128 ms. Because values associated with the first and last time windows could be affected by border problems the values of the first two and the last two time windows were excluded.

4. Results and discussion

4.1. Spontaneous EEG epochs

The quantifiers based on WE were used to examine short spontaneous EEG epochs recorded during open and closed eyes conditions. These two conditions were chosen as representing physiological brain states differing in their degree of EEG synchronization. It is well established that in closed eyes condition, the EEG is characterized with rhythmic high amplitude alpha activity (7–14 Hz) dominating over posterior (occipital and parietal) areas. Upon eyes opening, alpha activity is blocked (desynchronized) so that no dominant rhythm is evident in the EEG (Niedermeyer and Lopes da Silva, 1987). These changes in the rhythmic EEG organization manipulated by eyes opening and closing are expected to be reflected by WE measures at three electrodes (Fz, Cz, Pz, (Nunez, 1981, 2000)).

In this application, several issues were addressed, (i) to demonstrate the applicability of WE quantifiers to short (1 s) EEG epochs by comparing results with those obtained with longer (2 s) epochs; (ii) to compare the sensitivity of different WE quantifiers (temporal average and mean WE); (iii) to demonstrate the functional relevance of WE measures.

Derived WE quantifiers, $\langle S_{WT} \rangle$ and $\tilde{S}_{WT}$, were evaluated for the 1st and 2nd halves of a 2 s record, as well as for the whole 2 s epoch of spontaneous EEG records with eyes open and closed. These three intervals were denoted by $T_1 = (0, 1)$ s, $T_2 = (1, 2)$ s and $T_3 = (0, 2)$ s. Fig. 3a displays group means of relative wavelet energy and WE of the spontaneous EEG over time for Cz lead. For the open eyes condition, the main activity is in the theta and alpha bands whereas for the closed eyes condition, alpha frequency band is dominant. Accordingly, it is seen from the temporal evolution of WE illustrated in the figure that WE values are lower in the closed eyes condition, with the observations for Fz and Pz being similar.

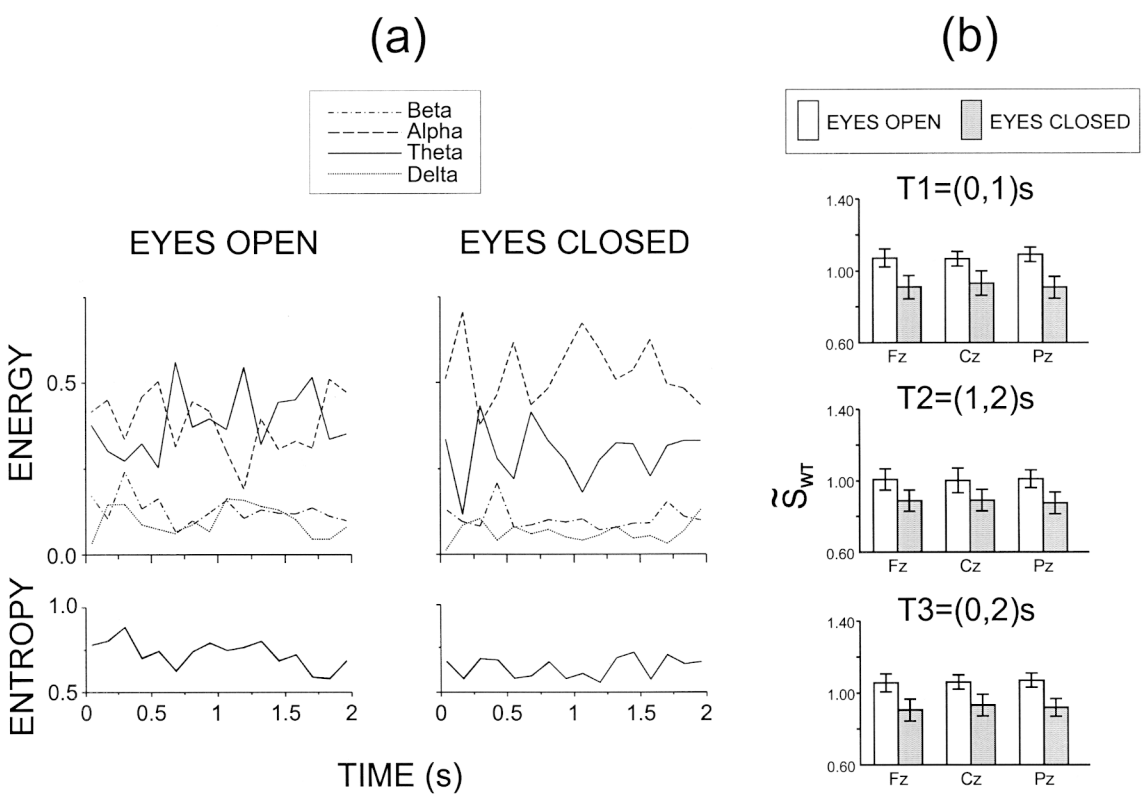

Fig. 3. Grand average of time evolution of relative wavelet energy and total WE at lead Cz in spontaneous EEG (2 s epoch) in open and closed eyes conditions (a); grand average of $\tilde{S}_{WT}$ (mean ± S.E.) of spontaneous EEG for $T_1 = (0, 1)$ s, $T_2 = (1, 2)$ s and $T_3 = (0, 2)$ s epochs in open and closed eyes conditions at Fz, Cz and Pz (b).

For statistical assessment, $\langle S_{WT} \rangle$ and $\tilde{S}_{WT}$ were evaluated for each of the three time intervals T_1, T_2 and T_3. They were subjected to a repeated measures analysis of variance with two within-subject variables *condition* (closed vs. open eyes) and *lead* (Fz, Cz, Pz).

4.1.1. Interval T_1

For $\langle S_{WT} \rangle$, there was a significant condition effect ($F(1/12) = 5.54$, $P < 0.05$), because the WE was significantly lower in the closed as compared with the open eyes condition (0.76 and 0.89, respectively). No significant lead effect was detected. Fig. 3b demonstrates that the same results were obtained for $\tilde{S}_{WT}$, with even stronger effect found for condition ($F(1/12) = 9.69$, $P < 0.01$).

4.1.2. Interval T_2

For $\langle S_{WT} \rangle$, the condition effect was detected as a trend ($F(1/12) = 3.68$, $P = 0.08$), with no inter-electrode differences found. In contrast the condition effect was significant for $\tilde{S}_{WT}$ ($F(1/12) = 6.93$, $P = 0.02$, Fig. 3b).

4.1.3. Interval T_3

For $\langle S_{WT} \rangle$, only a marginal condition effect was revealed ($F(1/12) = 4.12$, $P = 0.07$). In contrast, the effect of condition was highly significant for $\tilde{S}_{WT}$ ($F(1/12) = 9.11$, $P < 0.01$) as demonstrated in Fig. 3b.

Because T_1, T_2 and T_3 are physiologically identical, to exclude the possibility that the WE measures may capture nonphysiological effects, analysis of variance (ANOVA) design with two factors *time epoch* (T_1, T_2, T_3) and *lead* (Fz, Cz, Pz) was performed for $\langle S_{WT} \rangle$ and $\tilde{S}_{WT}$. No significant main effect or interactions were obtained for the time epoch variable, which verifies the physiologically based reactivity of the WE measures. In summary (i) WE measures for short (1 s) EEG epochs differentiated physiological brain states as effectively as for longer epochs; (ii) the difference between the two physiological conditions affecting the EEG synchronization (closed and open eyes) was better emphasized by $\tilde{S}_{WT}$; (iii) WE measures are physiologically meaningful.

4.2. Event-related potentials

Theoretically, RWE measures may be based on either spontaneous or pre-stimulus epochs. During task condition, the inter-trial EEG activity may be affected by task performance, which in turn may modify the relative quantifiers. To explore the possible effect of task performance on relative wavelet energy, WE measures from three time intervals for, (1) spontaneous EEG with closed eyes; (2) pre-stimulus EEG in a passive listening condition; and (3) pre-stimulus EEG in an active (simple reaction) task condition, were compared.

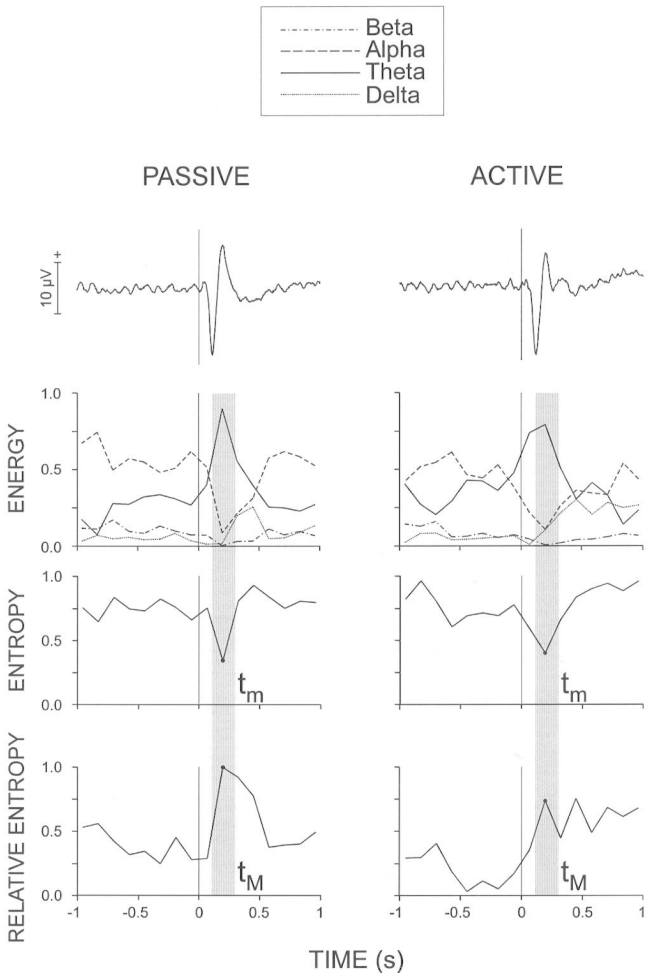

Fig. 4. EEG-ERP grand average and grand average of relative wavelet energy (ENERGY), total WE (ENTROPY) and RWE (RELATIVE ENTROPY) time evolutions in passive listening condition (PASSIVE, left panel) and simple reaction task (ACTIVE, right panel) conditions at Cz. $t = 0$ indicates for the moment of stimulus occurrence. Shadow columns represent the variation in the values of latencies t_m (minimum value of WE in the post-stimulus epoch) and t_M (maximum value of RWE in the post-stimulus epoch).

Statistical results showed that none of the WE measures differed among spontaneous, passive pre-stimulus, and active pre-stimulus epochs ($P > 0.1$ for all analyzes). Therefore, passive and task conditions do not produce significant difference in pre-stimulus WE measures. Nonetheless, this conclusion should be regarded as restricted to random stimulus conditions and a limited number of midline locations. It should be further explored if certain task conditions do not cause pre-stimulus WE effects at specific electrodes (Rockstroh et al., 1989; Birbaumer et al., 1990).

To quantify complex signal synchronization processes in ERPs, temporal evolution of WE was analyzed for passive and task ERPs. Grand average auditory ERPs at Cz are illustrated in Fig. 4. In the figure, group means of relative wavelet energy, WE and RWE as a function of time are also displayed. Relative

wavelet energies demonstrate that the alpha band activity is dominant in the pre-stimulus epochs. For both passive and task ERPs, theta activity is dominant in the early post-stimulus epoch with a maximum at around 180–200 ms. This is followed by increments in the delta and alpha bands. The time evolution of total WE presents a clear minimum also at around 180–200 ms for both the PLC and SRT. Note that the time evolution of the WE is in a very good agreement with the theoretical consideration given in Section 2.3, and the time at which it is minimal can be associated with a strong frequency tuning or highly synchronized activity in the theta band induced by the stimulus, resulting in a very ordered state. Fig. 4 also indicates that the highest degree of nonsimilarity between reference pre-stimulus EEG and ERP for both recording conditions manifests the same behavior, as also observed but not illustrated for Fz and Pz.

A two-way repeated-measures analysis of variance with within factors *condition* (PLC vs. SRT) and *lead* (Fz, Cz, Pz) was used to analyze statistically the WE quantifiers. For $\langle S_{WT} \rangle$ and $\tilde{S}_{WT}$, no effects of condition or lead were found.

Fig. 5 (left panel) demonstrates that t_m mean values (post-stimulus time point of minimal total WE) were overall shorter in the PLC (225 ms) than in the SRT (251 ms) condition, although these effects did not reach significance. It is also shown in the figure that the signal rate of WE change $\Gamma[t_m]$ was substantial (greater than 50%), indicating that at point t_m, the stimulus produced

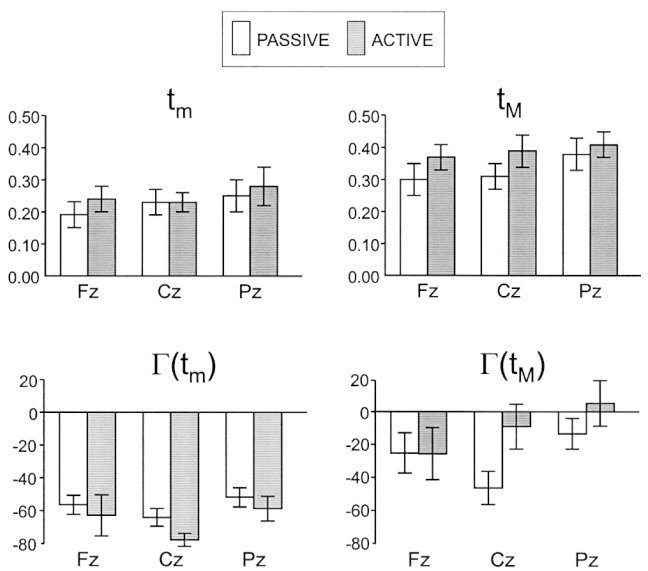

Fig. 5. Group means (mean ± S.E.) of t_m (minimum value of WE in the post-stimulus epoch) and t_M (maximum value of RWE in the post-stimulus epoch) for EEG-ERP in passive listening (PASSIVE) and simple reaction task (ACTIVE) conditions at Fz, Cz and Pz (upper panel); group means (mean ± S.E.) of signal rate of WE change evaluated for t_m and t_M in the same recording conditions (bottom panel).

a strong ordering in the signal in the two conditions. The WE decrease was significantly more pronounced at central (70%) than at frontal and parietal sites (56 and 52%), as indicated by the main lead effect ($F(2/24) = 3.83$, $P < 0.05$). Also, there was a trend for the task stimuli to produce a stronger decrease in WE (PLC = 57%, SRT = 66%).

Fig. 5 (right panel) demonstrates t_M mean values in the PLC (330 ms) and SRT (389 ms) conditions and shows that no reliable effects of the variables under study were obtained. For $\Gamma[t_M]$, there was a significant main effect of the lead factor because $\Gamma[t_M]$ was expressed at frontal–central, but not at the parietal location. Also, there was a marginal *condition* × *lead* interaction ($0.05 < P < 0.1$) because the frontal $\Gamma[t_M]$ were similar for passive and active stimuli, while the $\Gamma[t_M]$ was significantly less expressed for the active stimuli at central and parietal locations.

In Fig. 6, group mean wavelet energies of delta, theta, alpha and beta ($j = -6, \ldots, -3$) frequency bands in the pre-stimulus epoch are presented. The gamma energy contribution ($j = -2$) is negligible, and, therefore, is not displayed. At the three leads, the alpha band had a major contribution to the total wavelet energy. In the same figure, relative wavelet energies of the above frequency bands at t_m and t_M are shown. Comparing background relative wavelet energies with its latency at t_m, it is clear that stimulus major effect is a strong frequency tuning in the theta band, which produces a high degree of order in the signal as reflected by high negative signal rate of WE change $\Gamma[t_m]$. Looking at relative wavelet energies at latency t_M, a broad band distribution with pronounced contribution of the delta band, more strongly expressed in the SRT, is seen. In sum, these results demonstrate that: (i) WE quantifiers can localize temporally EEG signal ordering (synchronization) in the post-stimulus epoch. (ii) Stimulus effect can be viewed as a frequency tuning in given frequency bands. In the present study, this effect was persistent in the lower (theta) frequency band at 180–200 ms after stimulus. (iii) Scalp areas with maximal signal ordering can be clearly identified, even with small number of electrodes. (iv) Differences in processing conditions may be detected by means of WE measures.

5. Conclusion

The present paper describes the use of quantitative parameters derived from the orthogonal discrete wavelet transform applied for analysis of short duration brain electrical signals. The WE has the following advantages. (i) In contrast to spectral entropy, WE is capable of detecting changes in a nonstationary signal due to the localization characteristics of the wavelet

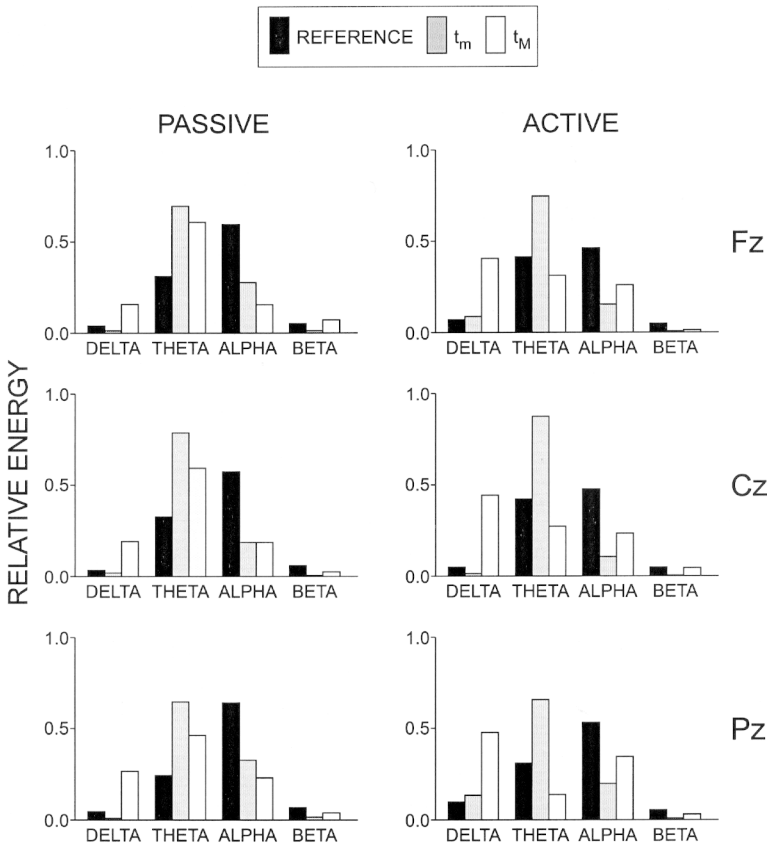

Fig. 6. Group means of relative wavelet energy of EEG frequency bands for pre-stimulus temporal average (REFERENCE) and, at latencies t_m and t_M, corresponding to EEG-ERPs recorded in passive (left panel) and active (right panel) conditions at Fz, Cz and Pz.

transform. (ii) In contrast to dimensions and Lyapunov exponents (which are only defined for stationary behaviors), or dimensionality and chaoticity measures (stationary constrains removed), the computational time of WE is significantly shorter since the algorithm involves the use of fast wavelet transform in a multiresolution framework. (iii) Contaminating noises (if they are basically concentrated in some frequency bands) contributions can be easily eliminated; and finally and very important. (iv) The WE is parameter-free.

Furthermore, the present results demonstrate that WE is physiologically meaningful since it differentiated specific physiological brain states under spontaneous or stimulus-related conditions. Significant decrease in the WE was observed in the post-stimulus epoch, indicating a more rhythmic and ordered behavior of the EEG signal compatible with a dynamic process of synchronization in the brain activity. In addition, time evolution parameters derived from WE can identify the time localizations of dynamic processes in the post-stimulus epochs.

As being independent of the amplitude or the energy of the signal, the WE gives a new information about EEG/ERP signals in comparison to the one obtained by using frequency analysis or other standard methods.

The use of the proposed quantifiers based on time–frequency methods (like ODWT) can contribute to the analysis of brain responses and may also lead to a better understanding of their dynamics. Certainly, the use of these quantifiers is not intended to replace conventional EEG/ERP analyzes, but to provide further insights into the underlying brain mechanisms.

Acknowledgements

This work was supported by the Consejo Nacional de Investigaciones Cientificas y Técnicas (CONICET), Argentina (PIP 0029/98), Fundación Alberto J. Roemmers, Argentina, the International Office of BMBF, Germany (ARG-4-G0A-6A), the Deutsche Forschungsgemeinschaft, Germany (436-BUL-113/105), and James McDonnell Foundation, USA (98-66 EE-GLO-04).

References

Abarbanel HDI. Analysis of Observed Chaotic Data. New York: Springer, 1996.

Aldroubi A, Unser M, editors. Wavelets in Medicine and Biology. Boca Raton: CRC Press, 1996.

Başar E. EEG-brain dynamics. Relation between EEG and Brain Evoked Potentials. Amsterdam: Elsevier, 1980.

Başar E. Brain Function and Oscillations (I): Brain Oscillations, Principles and Approaches. Berlin: Springer, 1998.

Başar E. Brain Function and Oscillations (II): Integrative Brain Function. Neurophysiology and Cognitive Processes. Berlin: Springer, 1999.

Birbaumer N, Elbert T, Canavan AG, Rockstroh B. Slow potentials of the cerebral cortex and behavior. Physiol Rev 1990;70:1–41.

Blanco S, Quian Quiroga R, Rosso OA, Kochen S. Time–frequency analysis of electroencephalogram series. Phys Rev E 1995;51:2624–31.

Blanco S, D'Attellis C, Isaacson S, Rosso OA, Sirne R. Time–frequency analysis of electroencephalogram series (II): gabor and wavelet transform. Phys Rev E 1996;54:6661–72.

Blanco S, Figliola A, Quian Quiroga R, Rosso OA, Serrano E. Time–frequency analysis of electroencephalogram series (III): wavelet packets and information cost function. Phys Rev E 1998;57:932–40.

Casdagli MC, Iasemedis LD, Savit RS, Gilmore RL, Roper SN, Sackellares JC. Non-linearity in invasive EEG recordings from patients with temporal lobe epilepsy. Electroenceph Clin Neurophysiol 1997;102:98–105.

Daubechies I. Ten Lectures on Wavelets. Philadelphia: SIAM, 1992.

Elbert T, Ray WJ, Kowalik ZJ, Skinner JE, Graf KE, Birbaumer N. Chaos and physiology: deterministic chaos in excitable cell assemblies. Physiol Rev 1994;74:1–47.

Gazzaniga MS, Ivry RB, Mangun GR. Cognitive Neuroscience: The Biology of the Mind. New York: WW Norton & Co, 1998.

Gray R. Entropy and Information Theory. New York: Springer, 1990.

Guiasu S. Information Theory with Applications. New York: McGraw-Hill, 1997.

Iasermedis LD, Sackellares JC. The evolution with time of spatial distribution of the largest Lyapunov exponent on the human epileptic cortex. In: Duke D, Pritchards W, editors. Measuring Chaos in Human Brain. Singapore: World Scientific, 1991:49–82.

Iasemedis LD, Sackellares JC, Zaveri HP, Williams WJ. Phase space topography and Lyapunov exponent of electrocorticograms in partial seizures. Brain Topogr 1990;2:187–201.

Inouye T, Shinosaki K, Sakamoto H, Toi S, Ukai S, Iyama A, Katzuda Y, Hirano M. Quantification of EEG irregularity by use of the entropy of power spectrum. Electroenceph Clin Neurophysiol 1991;79:204–10.

Inouye T, Shinosaki K, Imaya A, Matsumoto Y. Localization of activated areas and directional EEG patterns during mental arithmetic. Electroenceph Clin Neurophysiol 1993;86:224–30.

Lehnertz K, Elger CE. Can epileptic seizures be predicted? Evidence from nonlinear time series analysis of brain electrical activity. Phys Rev Lett 1998;80:5019–22.

Mallat S. A Wavelet Tour of Signal Processing, second ed. San Diego: Academic Press, 1999.

Niedermeyer E, Lopes da Silva FH, editors. Electroencephalography, Basic Principles, Clinical Applications, and Related Field. Baltimore: Urban & Schwarzenberg, 1987.

Nunez PL. Electric Fields of the Brain: The Neurophysics of EEG. New York/Oxford: Oxford University Press, 1981.

Nunez PL. Toward a quantitative description of large scale neocortical dynamic function and EEG. Behav Brain Sci 2000, in press.

Pjin JP, Van Neerven J, Noestt A, Lopes da Silva FH. Chaos or noise in EEG signals: dependence on state and brain site. Electroenceph Clin Neurophysiol 1991;79:371–81.

Powell CE, Percival IC. A spectral entropy method for distinguishing regular and irregular motion of Hamiltonian systems. J Phys A: Math Gen 1979;12:2053–71.

Quian Quiroga R., Rosso O.A., Başar E., Schürmann M. Wavelet-entropy in event-related potentials: A new method shows ordering of EEG-oscillations. Biol Cyber 2000a, in press.

Quian Quiroga R., Arnhold J., Lehnertz K., Grassberger P. Kullback-Leibler and renormalised entropy: applications to EEG of epilepsy patients. Phys Rev E 2000b, in press.

Rockstroh B, Elbert T, Canavan A, Lutzenberger W, Birbaumer N. Slow Cortical Potentials and Behaviour. Baltimore: Urban & Schwarzenberg, 1989.

Rosso OA, Blanco S. Characterization of dynamical evolution of electroencephalogram time series, 1999, unpublished.

Sayers B, Beagley HA, Riha J. The mechanism of auditory evoked EEG response. Nature 1974;247:481–3.

Shannon CE. A mathematical theory of communication. Bell Syst Technol J 1948;27:379–23, 623–56.